Weak rates for ECSN progenitor evolution and nucleosynthesis

Gabriel Martínez Pinedo

TECHNISCHE UNIVERSITÄT DARMSTADT

Electron Capture Supernova & Super-AGB Star Workshop,
Melbourne, February 1-6, 2016

Outline

Stellar Evolution Intermediate mass stars

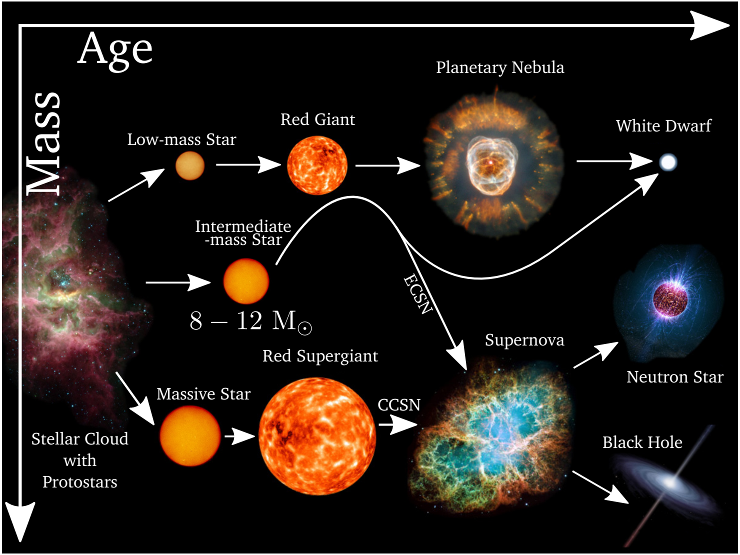

Core evolution (intermediate stars)

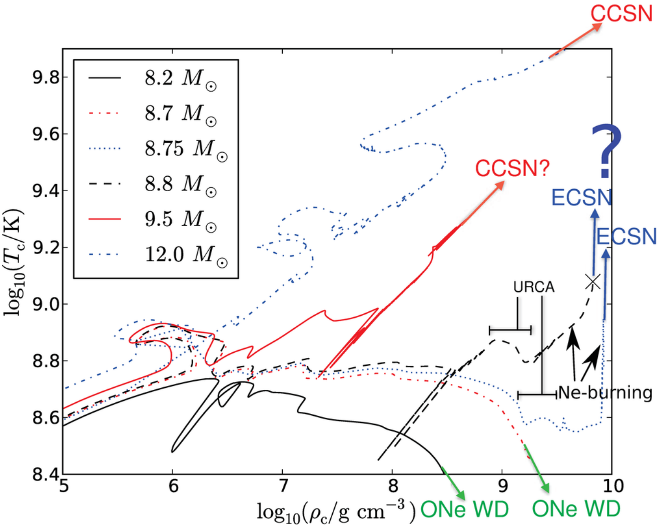

Jones *et al.*, ApJ **772**, 150 (2013)

Threshold densities for electron capture

TABLE 6.3
Threshold Density for Electron Capture

Nuc.	ϵ_0 (MeV)	$2Y_e\rho$ (g/cm^3)	*Nuc.*	ϵ_0 (MeV)	$2Y_e\rho$ (g/cm^3)
^{1}H	0.782	2.44×10^{7}	^{28}Si	4.643	1.97×10^{9}
^{3}He	0.0186	3.94×10^{4}	^{29}Si	3.681	1.05×10^{9}
^{4}He	20.6	1.37×10^{11}	^{30}Si	8.539	1.08×10^{10}
^{12}C	13.37	3.89×10^{10}	^{31}P	1.491	1.06×10^{8}
^{13}C	13.44	3.95×10^{10}	^{32}S	1.710	1.47×10^{8}
^{14}N	0.156	1.15×10^{6}	^{33}S	0.249	2.60×10^{6}
^{15}N	9.772	1.58×10^{10}	^{34}S	5.38	2.95×10^{9}
^{16}O	10.42	1.90×10^{10}	^{35}Cl	4.854	2.22×10^{9}
^{17}O	8.480	1.06×10^{10}	^{36}A	0.7096	1.99×10^{7}
^{18}O	14.06	4.51×10^{10}	^{37}Cl	0.1675	1.30×10^{6}
^{19}F	4.819	2.18×10^{9}	^{38}A	4.917	2.30×10^{9}
^{20}Ne	7.026	6.20×10^{9}	^{39}K	0.565	1.24×10^{7}
^{21}Ne	5.686	3.44×10^{9}	^{40}Ca	1.312	7.85×10^{7}
^{22}Ne	10.85	2.13×10^{10}	^{41}K	2.492	3.78×10^{8}
^{23}Na	4.374	1.67×10^{9}	^{42}Ca	3.521	9.34×10^{8}
^{24}Mg	5.513	3.16×10^{9}	^{44}Ca	5.659	3.39×10^{9}
^{25}Mg	3.833	1.17×10^{9}	^{48}Ti	3.990	1.30×10^{9}
^{26}Mg	9.325	1.38×10^{10}	^{52}Cr	3.976	1.29×10^{9}
^{27}Al	2.609	4.25×10^{8}	^{56}Fe	3.695	1.06×10^{9}

David Arnett, *Supernovae and Nucleosynthesis*

Urca pairs: cooling vs heating

mass parabola for isobaric chain

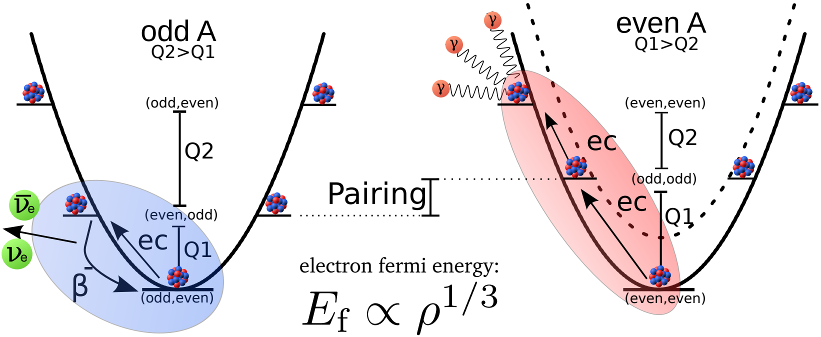

electron fermi energy:

$$E_\mathrm{f} \propto \rho^{1/3}$$

Urca cooling

$$(\mathrm{A,Z}) + e^- = (\mathrm{A,Z\text{-}1}) + \nu_e$$
$$(\mathrm{A,Z\text{-}1}) = (\mathrm{A,Z}) + e^- + \bar{\nu}_e$$

heating

$$(\mathrm{A,Z}) + e^- = (\mathrm{A,Z\text{-}1}) + \nu_e$$
$$(\mathrm{A,Z\text{-}1}) + e^- = (\mathrm{A,Z\text{-}2})^* + \nu_e + \gamma$$

Description electron capture and beta decay rates

Both rates are given by a thermal average over states in the initial nucleus:

$$\lambda = \frac{\sum_{if}(2J_i + 1)\lambda_{if} e^{-E_i/(kT)}}{\sum_i (2J_i + 1) e^{-E_i/(kT)}}$$

Allowed approximation (Gamow-Teller transitions)

$$\lambda_{if} = \frac{\ln 2}{K} B_{if} \Phi(q_{if}, \mu_e, T), \quad K = 6144 \text{ s}$$

- B_{if}: transition matrix element. Most of the relevant transitions are experimentally known. Shell-model calculations are possible.
- $\Phi(q_{if}, \mu_e, T)$: "trivial" phase space integral that accounts for the strong sensitivity of rates to temperature and density. Implementation in stellar evolution codes requires special care.

What to include in a weak interaction rate table?

- Directly the rates: Requires very fine grids in density and temperature to achieve accurate interpolations. Particularly relevant at the low temperatures relevant for ONeMg core evolution.
- Instead of the rate tabulate an effective matrix element (Fuller, Fowler and Newmann 1985). For electron capture

$$\lambda^{\text{ec}} = \frac{\ln 2}{K} B_{\text{eff}} \Phi^{\text{ec}}(q_{\text{gs}}, \mu_e, T), \qquad q_{\text{gs}} = Q_{\text{gs}}/(m_e c^2)$$

Phase space can be expressed via Fermi integrals:

$$\Phi^{\text{ec}}(Q, \mu_e, T) = \left(\frac{kT}{m_e c^2}\right)^5 \left\{F_4\left(\frac{\mu_e - Q}{kT}\right) + 2\frac{Q}{kT}F_3\left(\frac{\mu_e - Q}{kT}\right) + \left(\frac{Q}{kT}\right)^2 F_2\left(\frac{\mu_e - Q}{kT}\right)\right\}$$

Allows to use approximate expressions for Fermi integrals: fast and accurate up to 10-20%.

- An extension to β^- decay is necessary.

Example: Electron capture on ^{23}Na

Rates from Oda *et al* (1994) tabulation.

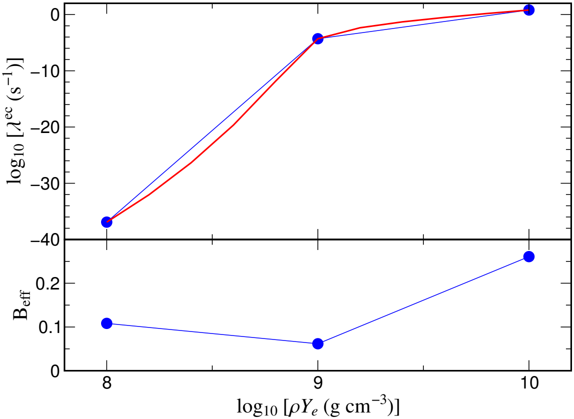

- Direct interpolation in sparse density grid results in 1-2 orders of magnitude uncertainty.
- Interpolation matrix element results in a maximum error of a factor 2.

How to do better?

In general, all rates relevant for ONeMg core evolution are determined by a few transitions. It is possible to provide analytical expressions for each individual rate [GMP+, PRC **89**, 045806 (2014)]

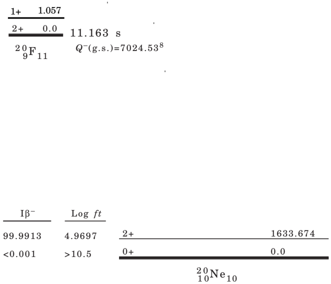

- Low densities (all temperatures): Rate determined by $2^+ \rightarrow 2^+$ ($Q = 5.902$ MeV) transition (experimentally known from beta decay).
- Intermediate densities ($T < 0.9$ GK): determined second forbidden transition $0^+ \rightarrow 2^+$ ($Q = 7.536$ MeV) (only an experimental limit)
- Higher densities: transition $0^+ \rightarrow 1^+$ ($Q = 8.592$ MeV determines rate (experimentally known from (p, n) charge exchange).

Electron capture on ^{20}Ne

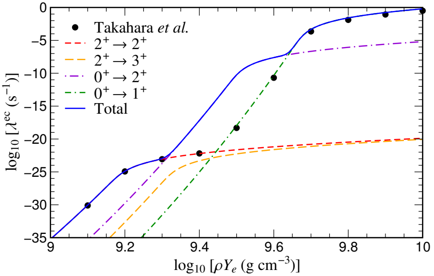

$T = 0.4$ GK

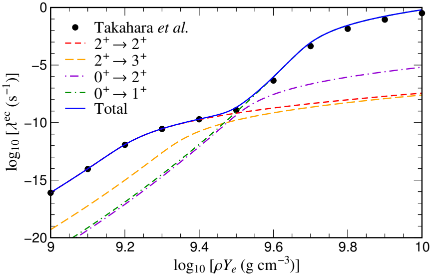

$T = 1$ GK

Mayor uncertainty is due to second forbidden transition.

Second forbidden calculation

$$\lambda = \frac{\ln 2}{K} \Phi^{\mathrm{2nd}}(q, \mu_e, T)$$

$$\Phi^{\mathrm{2nd}}(q, \mu_e, T) = \int_q^\infty wp(q+w)^2 C(w) F(Z, w) f_e(w, \mu_e, T) dw$$

- $C(w)$ is the shape factor: Linear combination of matrix elements and energy factors.
- Relevant matrix elements (Behrens & Bühring 1971)

$$\begin{aligned}
{}^V F_{211} &\sim \left[\boldsymbol{r} \otimes \boldsymbol{p}_{if}\right]^2 t_+, \quad \boldsymbol{p}_{if} = (\boldsymbol{p}_i + \boldsymbol{p}_f)/2 \\
{}^V F_{220} &\sim r^2 \boldsymbol{Y}_2 t_+ \\
{}^A F_{221} &\sim r^2 \left[\boldsymbol{Y}_2 \otimes \boldsymbol{\sigma}\right]^2 t_+
\end{aligned}$$

Shell-model calculations

sd-shell shell-model calculation using USDB interaction (Idini, Brown, Langanke, GMP, in preparation)

	Harmonic Oscillator	Wood–Saxon
${}^{V}F_{211}$	0.	0.0048
${}^{V}F_{220}$	0.8035	1.3353
${}^{A}F_{221}$	0.2423	0.3257

The beta-decay theoretical matrix element is $B = \langle C(w) \rangle = 1.36 \times 10^{-7}$ using $g_A = 1.27$ $(1.11 \times 10^{-7}$ for $g_A = 1.0)$.

The experimental upper limit is 1.94×10^{-7}.

Impact on electron capture and beta decay

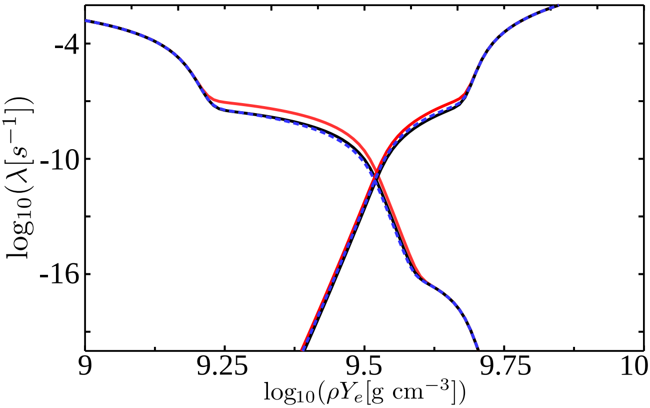

Blue dashed: Experimental limit

Red: Wood-Saxon wave functions

Black: Harmonic oscillator wave functions

Screening of weak interaction rates

The pressence of a degenerate electron background can affect both beta-decays and electron capture rates:

- Correction to nuclear binding energy (DeWitt, Graboske, and Cooper 1973; Hix and Thielemann 1996, Bravo and García-Senz 1999, Juodagalvis *et al.* 2010). Q-value increases by 0.1–0.3 MeV.
- Correction to electron energy (Itoh *et al.* 2002). Chemical potential reduced by 0.02–0.05 MeV.
- Net effect is a reduction of electron capture rate and an increase of the beta-decay rate.

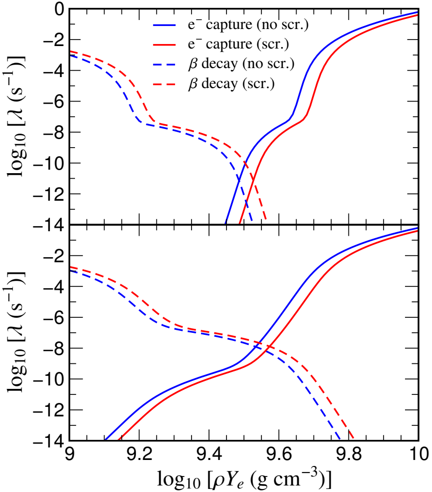

Having an analytical scheme allows to consider screening corrections consistent with the underlying EoS.

Impact evolution core

Based on ONeMg cores from Schwab, Quataert, and Bildsten 2015.
Convection does not develop in the core.

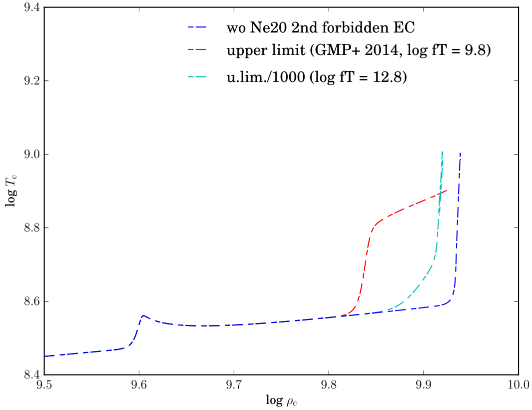

How sensitive is this result to the set of nuclear reactions included?

Larger network

Möller, Jones, GMP, in preparation

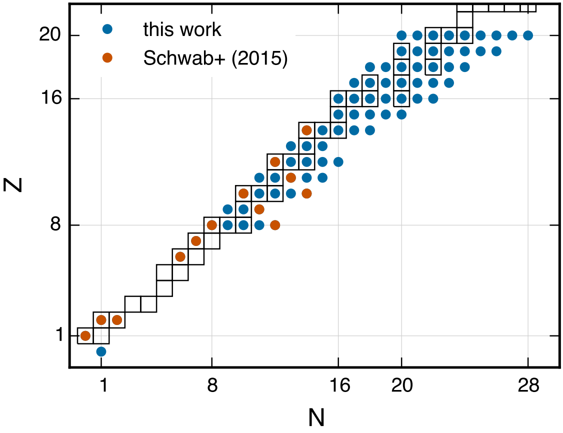

Increased to account for possible role of $^{20}\mathrm{O}(\alpha, n)^{23}\mathrm{Ne}$. This rate dominates over $^{20}\mathrm{Ne}(\alpha, \gamma)^{24}\mathrm{Mg}$ during Neon burning.

Evolution larger network

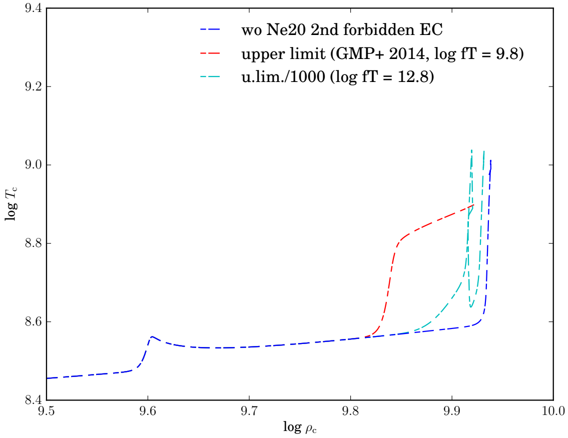

Convection does in fact develops in some of the models.

Evolution larger network

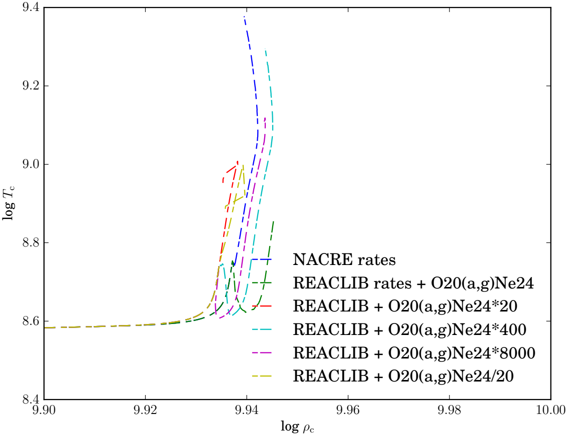

Evolution very sensitive to variations of $^{20}\mathrm{O}(\alpha, n)^{23}\mathrm{Ne}$ rate. It may affect the density at which oxygen deflagration initiates.

O DEFLAGRATION

MULTI-DIMENSIONAL SIMULATIONS

Joes, Röpke, Pakmor, Seitenzahl, Ohlmann, Edelmann, arXiv:1602.05771 [astro-ph.SR]

LEAFS code (Reinecke+ 1999, Röpke & Hillebrandt 2005, Röpke 2005, 2006)

Isothermal ONe core/WD in HSE with a **range of central (ignition) densities**

Centrally-confined ignition: 300 'bubbles' within 50 km sphere, < $5 \times 10^{-4}\, M_{\odot}$ inside initial flame surface

In **laminar regime**, flame speeds from **Timmes+ (1992)**; in **turbulent regime**, flame speeds from **subgrid scale model of turbulence (Schmidt+ 2006)**

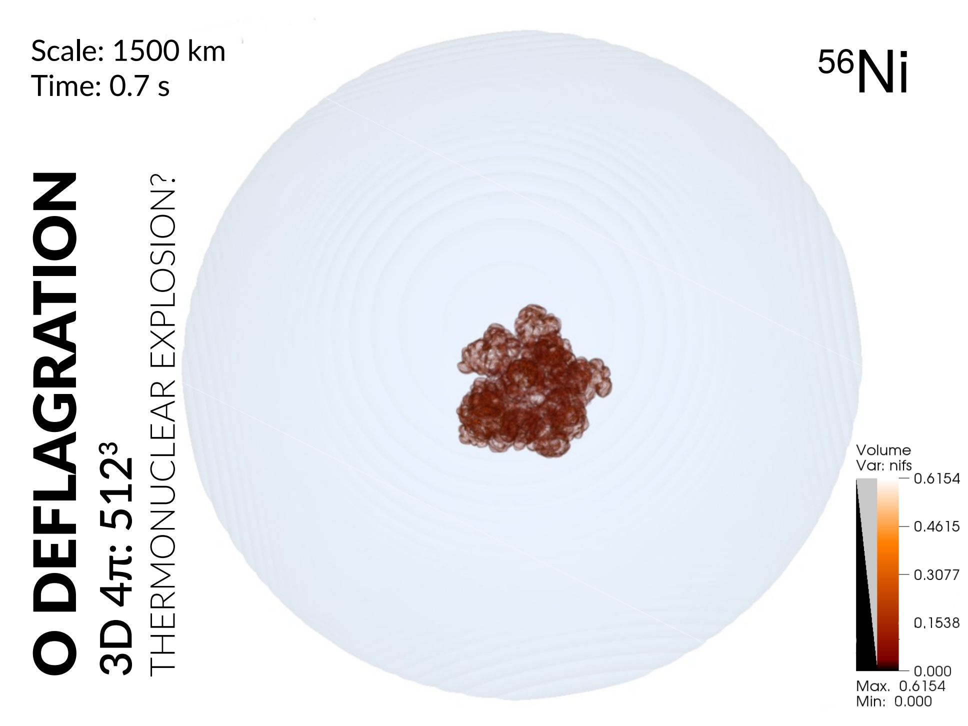
Scale: 1500 km
Time: 0.7 s
^{56}Ni
O DEFLAGRATION
3D 4π: 512^3
THERMONUCLEAR EXPLOSION?
Volume
Var: nifs
0.6154
0.4615
0.3077
0.1538
0.000
Max. 0.6154
Min: 0.000

Scale: 2500 km
Time: 1.3 s

O DEFLAGRATION

3D 4π: 512^3

THERMONUCLEAR EXPLOSION?

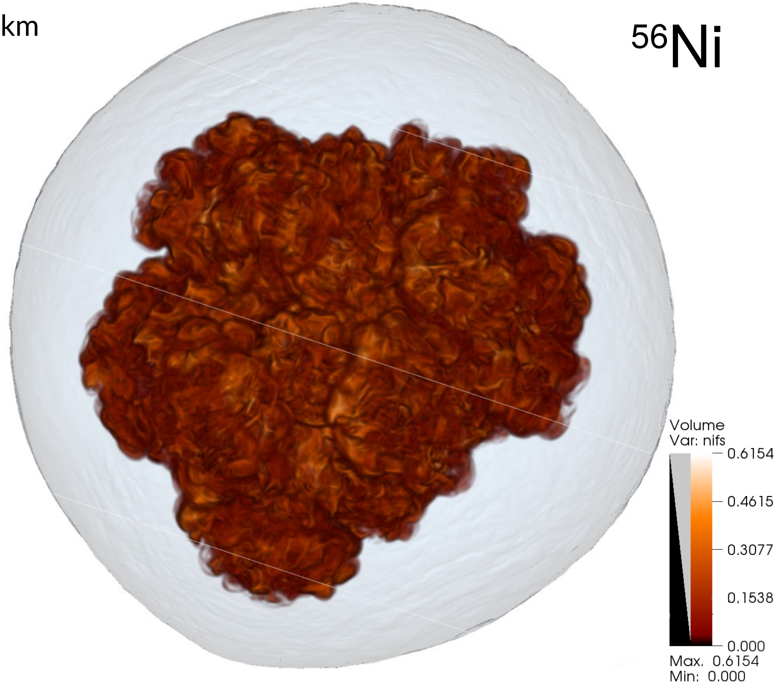

Scale: 400,000 km
Time: 60 s

^{56}Ni

O DEFLAGRATION

3D 4π: 512^3

THERMONUCLEAR EXPLOSION?

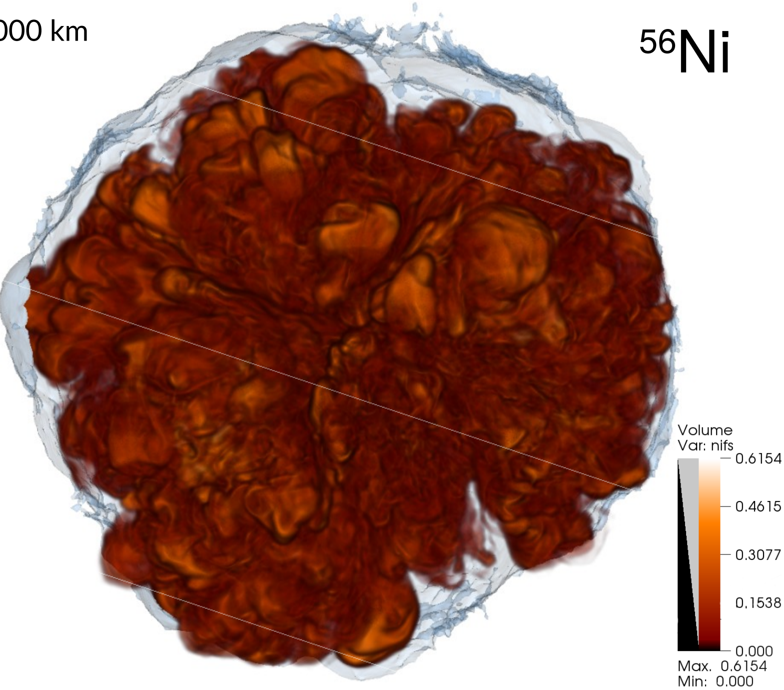

$\rho_{ign} = 10^{9.9}$ g cm^{-3}

THERMONUCLEAR EXPLOSION?

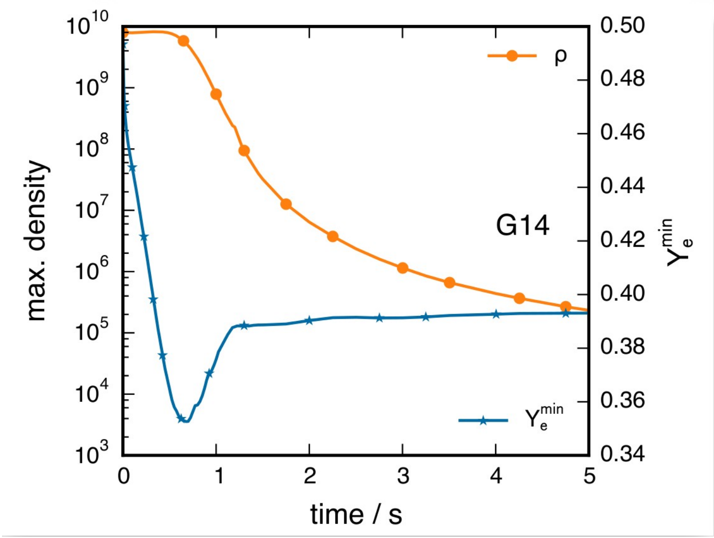

$\rho_{ign} = 10^{10.2}$ g cm^{-3}

CORE COLLAPSE

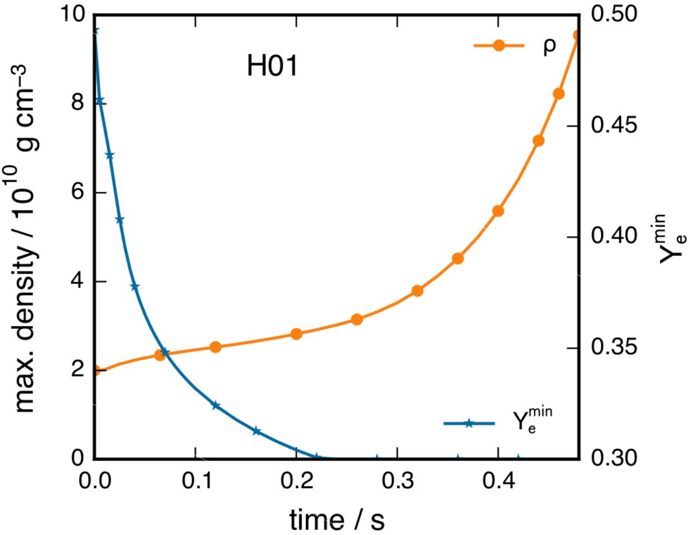

Heavy elements and metal-poor stars

Cowan & Sneden, Nature **440**, 1151 (2006)

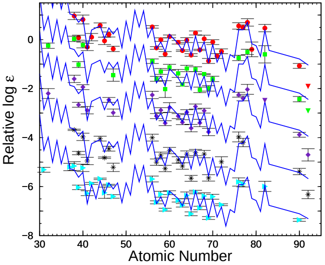

- Stars rich in heavy r-process elements ($Z > 50$) and poor in iron (r-II stars, $[\mathrm{Eu/Fe}] > 1.0$).
- Robust abundance patter for $Z > 50$, consistent with solar r-process abundance.
- These abundances seem the result of events that do not produce iron. [Qian & Wasserburg, Phys. Rept. **442**, 237 (2007)]
- Possible Astrophysical Scenario: Neutron star mergers.

- Stars poor in heavy r-process elements but with large abundances of light r-process elements (Sr, Y, Zr)
- Production of light and heavy r-process elements is decoupled.
- Astrophysical scenario: neutrino-driven winds from core-collapse supernova

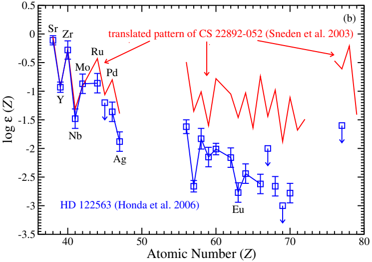

Honda *et al*, ApJ **643**, 1180 (2006)

Nucleosynthesis in neutrino-driven winds

Main processes:

$$\nu_e + n \rightleftarrows p + e^-$$
$$\bar{\nu}_e + p \rightleftarrows n + e^+$$

Neutrino interactions determine the proton to neutron ratio.

Neutron-rich ejecta:

$$\langle E_{\bar{\nu}_e}\rangle - \langle E_{\nu_e}\rangle > 4\Delta_{np} - \left[\frac{L_{\bar{\nu}_e}}{L_{\nu_e}} - 1\right]\left[\langle E_{\bar{\nu}_e}\rangle - 2\Delta_{np}\right]$$

- neutron-rich ejecta: r-process
- proton-rich ejecta: νp-process

We need accurate knowledge of ν_e and $\bar{\nu}_e$ spectra

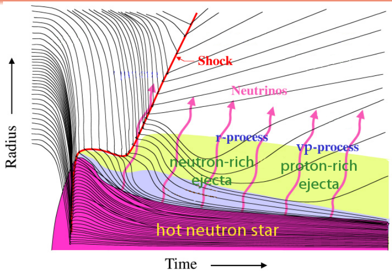

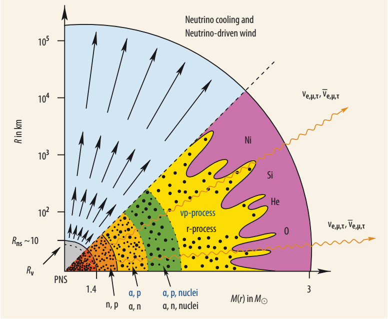

Weak rates in the decoupling region

Neutrino mean-free paths at high densities:

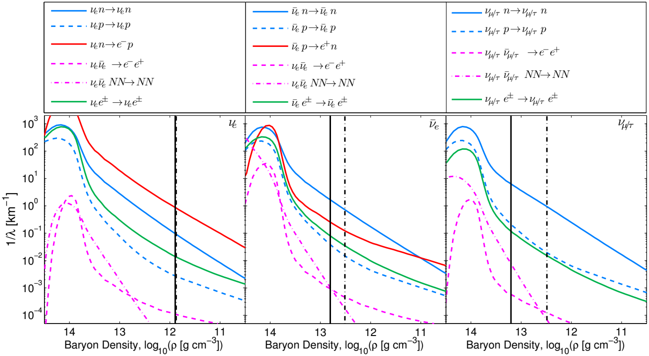

- ν_e emission: mainly determined by charged-current $\nu_e + n \rightleftarrows p + e^-$. Depends on equation of state properties.
- $\bar{\nu}_e$ emission: strong sensitivity to the processes considered and equation of state properties.

GMP, Fischer, Huther, J. Phys. G **41**, 044008 (2014)

Neutrino interactions at high densities

Most of Equations of State treat neutrons and protons as "non-interacting" (quasi)particles that move in a mean-field potential $U_{n,p}(\rho, T, Y_e)$.

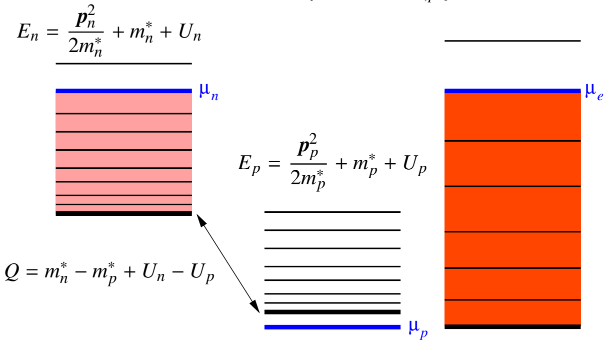

- Energy difference between neutrons and protons is directly related to nuclear symmetry energy.
- Symmetry energy enhances ν_e absorption and suppresses $\bar{\nu}_e$ absorption.
- Symmetry energy determines the spectral differences between ν_e and $\bar{\nu}_e$ and consequently the nucleosynthesis.

GMP, Fischer, Lohs, Huther, PRL **109**, 251104 (2012)
Roberts, Reddy, Shen, PRC **86**, 065803 (2012)

Constrains in the symmetry energy

- Combination nuclear physics experiments and astronomical observations (Lattimer & Lim 2013)
- Isobaric Analog States (Danielewicz & Lee 2013)
- Chiral Effective Field Theory calculations (Drischler+ 2014)

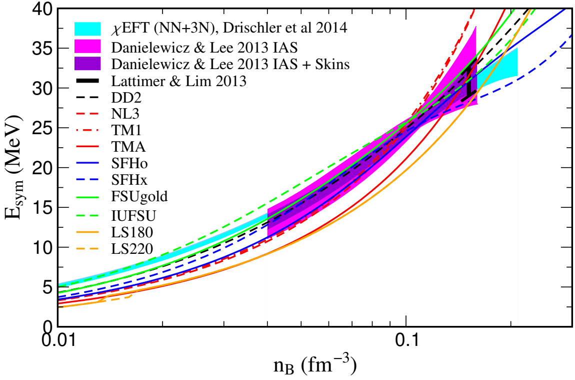

Figure data from Matthias Hempel (Basel)

Impact on neutrino luminosities and Y_e evolution

1D Boltzmann transport radiation simulations (artificially induced explosion) for a 11.2 $M_\odot$ progenitor based on the DD2 EoS (Stefan Typel and Matthias Hempel).

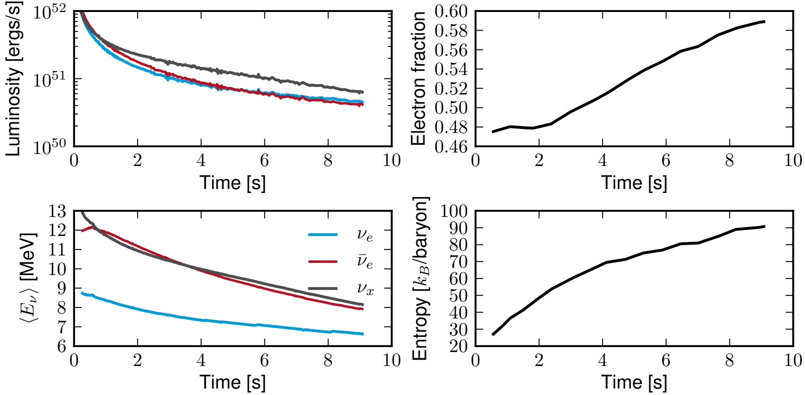

Y_e is moderately neutron-rich at early times and later becomes proton-rich.

GMP, Fischer, Huther, J. Phys. G **41**, 044008 (2014).

Nucleosynthesis

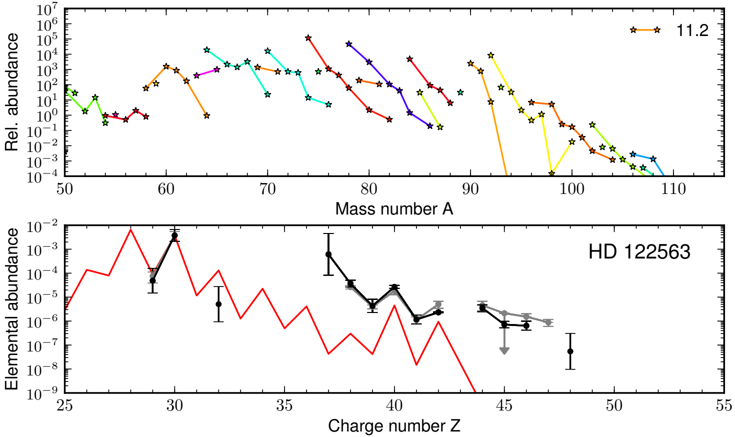

- Elements between Zn and Mo ($A \sim 90$) are produced
- Mainly neutron-deficient isotopes are produced
- Uncertainties: Equation of State, neutrino reactions (mainly $\bar{\nu}_e$), Neutrino oscillations(?).

Neutron decay

The neutron-proton energy difference in the medium could be of the order of several 10s MeV. Neutron decay is important for low energy neutrinos.

$$\bar{\nu}_e + p \rightleftarrows n + e^+$$

$$\bar{\nu}_e + e^- + p \rightleftarrows n$$

This is part of the direct URCA process in neutron stars [Lattimer *et al*, (1991)]

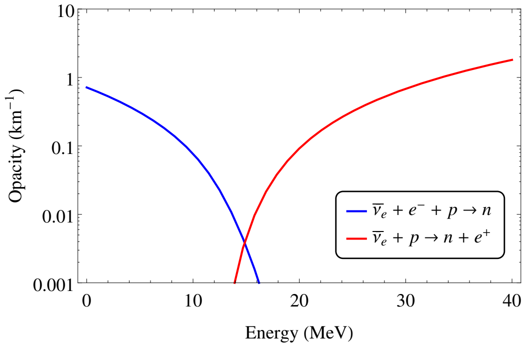

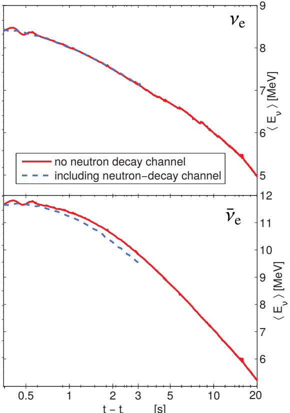

Fischer, Lohs, GMP, Qian, in preparation

Additional opacity channels for $\bar{\nu}_e$

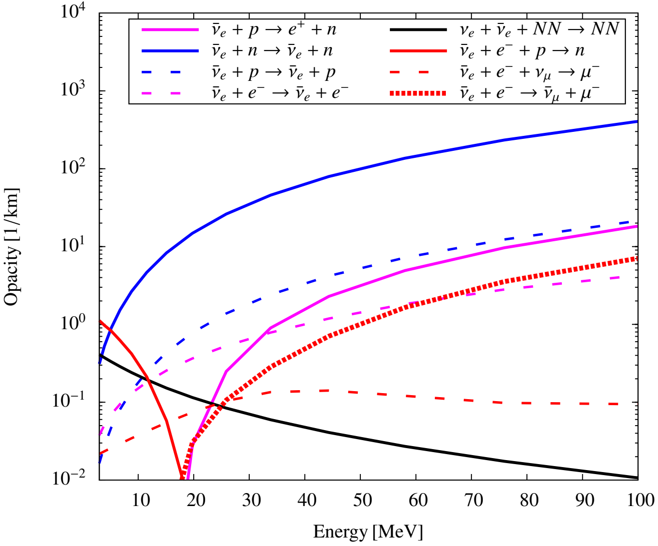

Summary

- Most of the weak interaction rates relevant for ONeMg cores evolution are well constrained by experimental data.
- Challenge: accurate and fast implementation of rates in stellar evolutionary codes.
- Core evolution sensitive to weak rates and thermonuclear rates.
- Final outcome sensitive to density of oxygen ignition. 3D simulations by Jones *et al*
- Electron capture supernova constitute an ideal test ground to explore the impact of neutrino opacities on heavy element nucleosynthesis.
- It is important to improve the description of $\bar{\nu}_e$ opacities in transport codes.